Penetration of an Initially Radial Shock Wave Through an Aluminum-Glass Interface[1]

B. A. SODEK, JR. and F. C. TODD, Department of Physics
Oklahoma State University, Stillwater

Introduction and Statement of the Problem

This paper presents an analytical study and computer solution for the propagation of an initially radial shock wave in aluminum through a plane interface into glass. The problem originates from the investigation of micrometeoroid impacts on photomultiplier tubes flown on space vehicles. Micrometeoroids are arbitrarily defined as particles with a mass of less than 10^{-4} grams. Theoretical considerations indicate that these particles may impact on the space vehicle with velocities in the range from 30,000 to 240,000 feet per second (Collins, 1960). There is a lower limit on the mass of these particles of about 10^{-16} grams because of the Poyting-Robertson effect (Beard, 1961). This effect predicts that the radiation from the sun will push very small particles outside the orbit of the earth. A typical micrometeoroid may be assumed to have a mass of 10^{-9} grams and a velocity of 118,000 feet per second. According to Whipple, some micrometeoroids with a relative density of 0.05 are presumably aggregates of material from the tails of comets. The densities of micrometeoroids appear to vary rather continuously from this low density up to that of iron-nickel with a relative density of 8.0. A stone meteoroid would have a density of about 4. The following calculation is not applicable for the very low density micrometeoroids.

Experiments have been reported in which simulated micrometeoroids are made to impinge at different velocities on a target. The penetration of high velocity projectiles produces craters which are very nearly hemispherical in shape and which show no apparent evidence of shear. Interpretation of available data suggests basic hydrodynamic theory as the first approximation to represent the cratering mechanism (Todd, 1960). It is useful because it permits an analytical study to be made and the results to be compared with experiment.

A typical crater from the impact of a glass sphere on an aluminum plate is shown in cross-section in Fig. 1. The initial velocity of the glass sphere was 28,500 feet per second. This slide was prepared in order to show the relatively uniform thickness of the plastically deformed crystals around the crater. The surface of the cavity under the projectile material is quite smooth. This is evidence of plastic flow of the target material during impact (Summers, 1959).

The basic assumption for the present calculation follows from such experimental evidence. The impacting micrometeoroid is assumed to initiate a radial shock wave in the aluminum which propagates away from the point of impact as a hydrodynamic shock wave in a non-viscous fluid. The nature of the physical processes during the initial phases of impact is not well understood; and consequently, the true conditions at the time of contact between micrometeoroid and target cannot be specified for an accurate analytical solution. The proposed problem is solved, however, with approximate initial conditions in order to obtain information that will assist in evaluating the relative importance of other possible mechanisms and to provide a basis for a more exact solution when the true

[1]Supported by National Aeronautics and Space Administration Contract No. NASr-7 administered through the Research Foundation, Oklahoma State University.

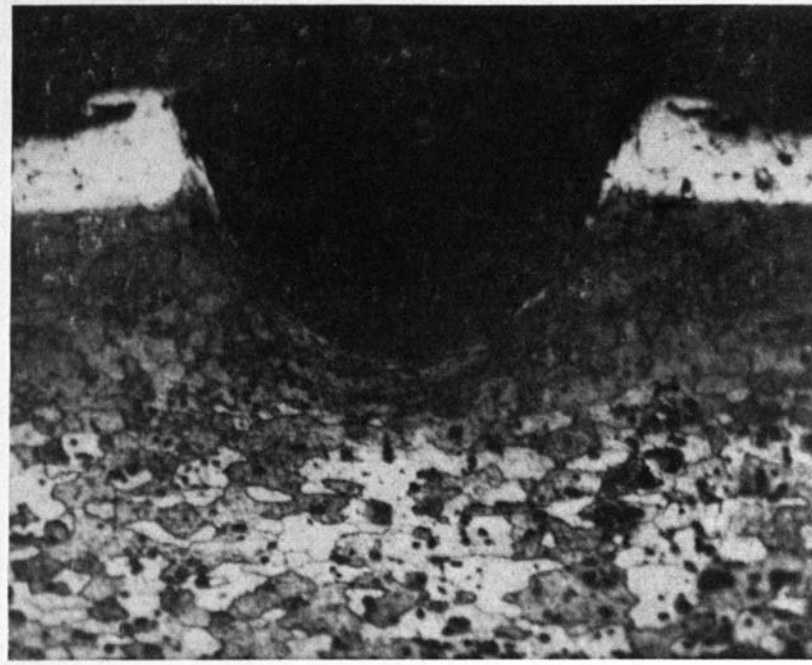

Fig. 1. Crater Formed by a Glass Missile Impacting at 28,000 Feet Per Second.

delineating conditions are known. As the shock moves from aluminum into glass, the prime interest for this calculation is the reflection and penetration of this wave at a plane interface. The interface moves during the impact, which differentiates the problem from the common seismic problem of reflection at an interface between two different media.

HYDRODYNAMIC EQUATIONS AND CONDITIONS

The pressure drop across a shock front is very much greater than the elastic limits of either aluminum or glass. Under these conditions, Bjork (1958) and others have assumed that the shock front is propagated as a hydrodynamic wave through a non-viscous fluid which may be described by the equations of fluid flow. These differential equations may be expressed in Eulerian or Lagrangean form. The Eulerian equations are written with respect to fixed space coordinates. The Lagrangean equations describe the motion in terms of the paths of motion of individual particles. In problems with two spatial coordinates and particularly for a multilayer target, the Eulerian form of the equations is perferred in order to simplify the calculations on a digital computer. The hydrodynamic differential equations, in Eulerian coordinates, are presented in Fig. 2. The origin of each equation is indicated.

Bethe (1942) has shown that the propagation of a shock wave through any medium can be solved provided the equation of state is known for each distinct material considered. In addition to the application of these equations, Hugoniot showed that the entropy must increase across the shock front. These two equations are presented in Fig. 3. The formal repre-

Conservation of Mass

$$\frac{\partial \rho}{\partial t} = - \frac{\partial (r\rho u)}{r\partial r} - \frac{\partial (\rho w)}{r\partial \theta} \qquad (1)$$

Conservation of Momentum

$$\frac{\partial (\rho u)}{\partial t} = - \frac{\partial p}{\partial r} - \frac{\partial (r\rho uu)}{r\partial r} - \frac{\partial (\rho wu)}{r\partial \theta} \qquad (2)$$

$$\frac{\partial (\rho w)}{\partial t} = - \frac{\partial p}{r\partial \theta} - \frac{\partial (r\rho uw)}{r\partial r} - \frac{\partial (\rho ww)}{r\partial \theta} \qquad (3)$$

Conservation of Energy

$$\frac{\partial (\rho E)}{\partial t} = - \frac{\partial (rpu)}{r\partial r} - \frac{\partial (\rho w)}{r\partial \theta} - \frac{\partial (r\rho uE)}{r\partial r} - \frac{\partial (\rho wE)}{r\partial \theta}$$

ρ	density	u	radial velocity
p	pressure	w	tangential velocity
E	internal energy	t	time
r	radial coordinate		
θ	angular coordinate		

Fig. 2. Hydrodynamic Flow equations in Polar Coordinates.

sentation is the same for either aluminum or glass. The last relation in this figure may be derived from the conservation equations and is the Rankine-Hugoniot energy equation. This expression relates the internal energy, pressure, and specific volume at the crest of a shock front to the corresponding values for the material which is yet undisturbed. The shock pressure-volume relationship of a given material is unique and is called the Hugoniot equation of state. A comprehensive equation of state is not immediately available for either material.

The Mie-Grüneisen (Grüneisen, 1926) equation of state is one of the most general relations possible. It relates pressure, volume and energy at points in *P, V,* and *E* space to the values of P_H, V_H and E_H on the Hugoniot curve. For both materials, experimental information is available for the low, less than one megabar, pressure region (Wackerle, 1962; Walsh, 1958.) Theoretical predictions, available from the use of the Thomas-Fermi statistical method, claim validity when pressures exceed twenty megabars.

Equation of State in Gruneisen Form

$$P - P_H = \gamma\rho\,(E - E_H) \tag{5}$$

Condition across Shock Front

$$S(\text{entropy}) \geq 0 \tag{6}$$

Rankine-Hugoniot Relation (Derived)

$$(E_H - E_0) = \tfrac{1}{2}(P_H - P_0)(V_0 - V_H) \tag{7}$$

P,V and E are pressure, volume, and internal energy
subscript 0 is in front of shock
subscript H is peak, or minimum values in the shock front.
γ is the Gruneisen ratio and changes slowly with the density, only.

Fig. 3. Additional Equations for Solution of Shock Propagation.

Adequate representation between these two extremes is made possible by interpolation. Equation of state curves for aluminum and glass appear in Figs. 4 and 5. The heavy line in each figure is the Hugoniot curve along which the material is compressed by a shock wave. The lighter curves are typical adiabats along which the material expands after it has been compressed by the shock front.

NUMERICAL SOLUTION OF FLOW EQUATIONS

To obtain a numerical solution on a digital computer, von Neumann and Richtmyer (1950) suggest that the differential equations be modified by the introduction of a pseudo-viscosity term. As a consequence, the shock front changes from a true discontinuity to a narrow zone of large gradients. The explicit form of the dissipative term in this problem is based on a suggestion by Landshoff (1955). This term is taken as q, and is given by Equation 8 in Fig. 6. This pseudo-viscosity term is added to the pressure, p, in the preceding differential equations expressing conservation of momentum and energy. The modified equations also appear in Fig. 6.

For convenience in scaling numerical magnitudes for a computer calculation and to preserve computer storage, the relevant equations are converted to a nondimensional form. A dimensionless solution also permits scaling to problems involving different impacting velocities and different sizes of particles. The resulting equations are then transformed to finite difference equations by methods similar to those used by Longley (1959) for cylindrical coordinates and prepared for solution by a digital computer.

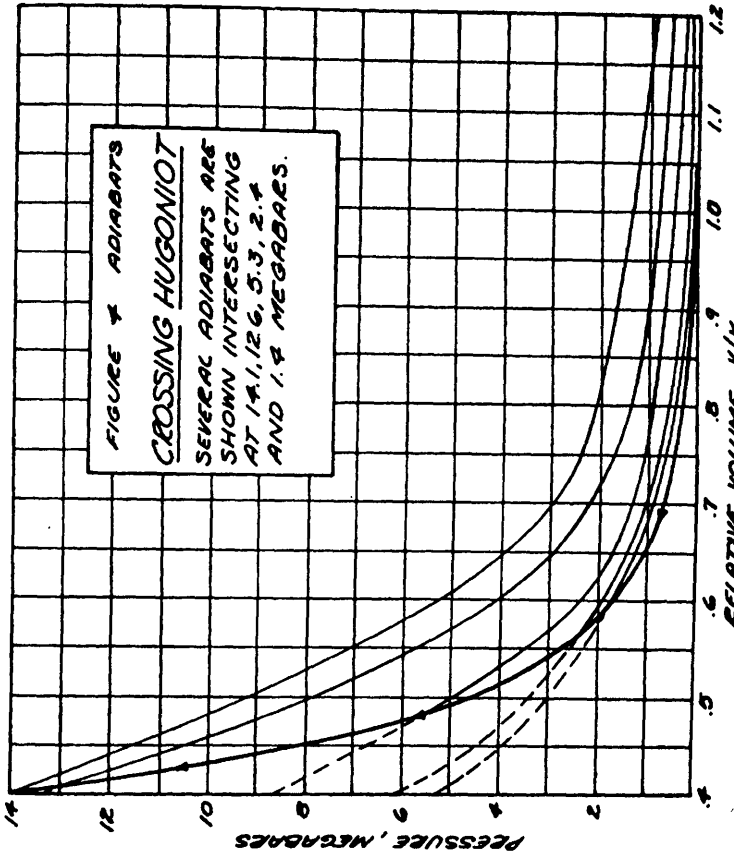

Fig. 4. Adiabats Crossing Hugoniot.

Boundary Conditions and Solutions

The finite difference equations yield a solution by the usual iterative method employed with digital computers. To apply these equations, conditions at time, t, equal zero must be completely specified. The assumption that a micrometeoroid produces a radial shock is illustrated in Fig. 7. The lower part of the figure shows the initial pressure distribution and the modified profile produced by the q term which permits a numerical method of solution. This pressure is 14.1 megabars, or a little over 14 million atmospheres, developed by the typical micrometeoroid of 10^{-6} grams impacting with an initial velocity of 118,000 feet per second. The radius of the shock front is 13 per cent greater than the radius of the micrometeoroid (Todd, 1961).

At later times, the shock wave propagates in aluminum and decreases in amplitude as the energy of the shock is spread over greater areas. After the shock radius has become about one-fifth greater than its initial value, the shock front encounters the aluminum-glass interface. The pressure and the particle velocity are continuous across the material

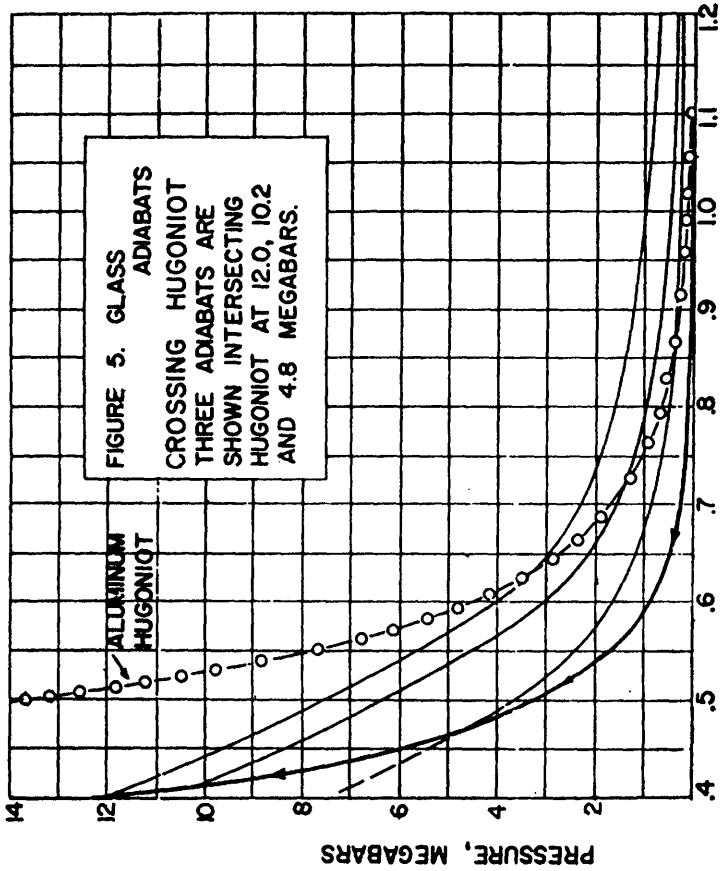

Fig. 5. Glass Adiabats Crossing Hugoniot

boundary; but the density and the intenal energy are discontinuous. The introduction of material of a different density destroys the radial symmetry of the flow. Fig. 8 illustrates density-radial distance curves at three different times. The ratio of the density to the normal aluminum density of 2.785 grams per cubic centimeter is indicated on the vertical axis. For example, at the start of the calculation, the density of the shocked aluminum is 7.32 grams per cubic centimeter which is approximately two and one-half times normal aluminum density. The top third of the figure shows the initial profile and a profile after 48 iteration cycles. The shock wave has not yet encountered the interface and the profile is identical along any radius. In the center graph, the leading point of the shock wave on the 90° line has reached the interface. The shock front is penetrating the interface and the building of a shock wave in the glass can be noted. A profile along the 5° line is also shown. Here, the disturbance is entirely in aluminum. The bottom portion of the figure again show profiles on the 5° and 90° radial lines after 96 cycles. The strength of the shock in glass has increased while the strength of the shock in

Dissipative term which is significant only for large velocity gradients

$$q = -A_1^2 (\text{div } \vec{V}) \rho (|\text{div } \vec{V}| + A_2) \tag{8}$$

when $\vec{V}$ is the material velocity vector, A_1 and A_2 are constants determined by trial and error.

Conservation of Momentum

$$\frac{\partial(\rho u)}{\partial t} = - \frac{\partial(p+q)}{\partial r} - \frac{\partial(r\rho uu)}{r\partial r} - \frac{\partial(\rho wu)}{r\partial \theta} \tag{9}$$

$$\frac{\partial(\rho w)}{\partial t} = - \frac{\partial(p+q)}{r\partial \theta} - \frac{\partial(r\rho uw)}{r\partial r} - \frac{\partial(\rho ww)}{r\partial \theta} \tag{10}$$

Conservation of Energy

$$\partial(\rho E) = - \frac{\partial[r(p+q)u]}{r\partial r} - \frac{\partial[(p+q)w]}{r\partial \theta} - \frac{\partial(r\rho uE)}{r\partial r} - \frac{\partial(\rho wE)}{r\partial \theta} \tag{11}$$

Fig. 6. Introduction of Viscous Damping Term for Integration Across Shock.

aluminum has decreased. The density of the material immediately behind the interface is lower than on the 5° line. This indicates the probability of a rarefaction wave being propagated back into the aluminum as a result of shock reflection at the interface. The interface has moved outward as the shock front passes. The old and new positions of the dividing line between aluminum and glass have been marked in the figure.

The behavior of the internal energy is similar to that of the density. The velocity and pressure are continuous across the material boundary and profiles of these variables have the same general character as those of the density front in aluminum. Calculations are in progress on later phases of this problem.

The assumed radial shock front resulting from the impact of a micrometeoroid on a multilayer target has been propagated through the aluminum layer and made to impact on the aluminum-glass interface. The incident shock front produces a transmitted shock wave in the glass and a reflected rarefaction wave traveling back into the aluminum.

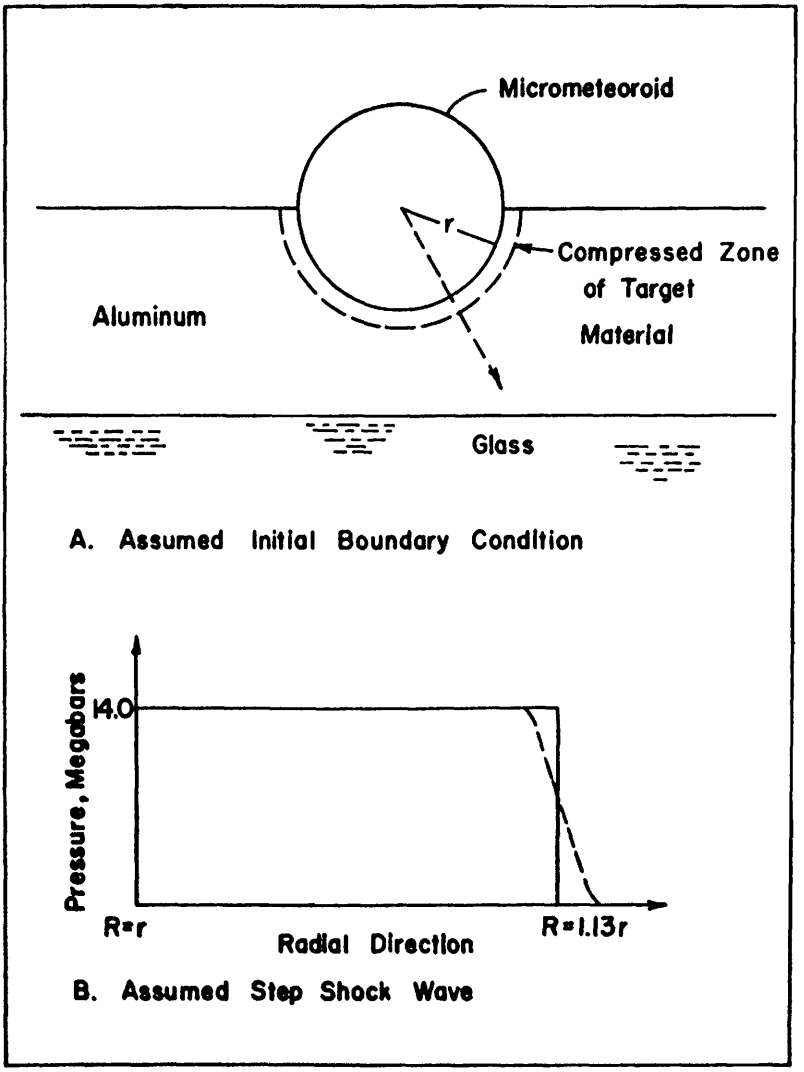

Fig. 7. Assumptions for Impact of a Sphere

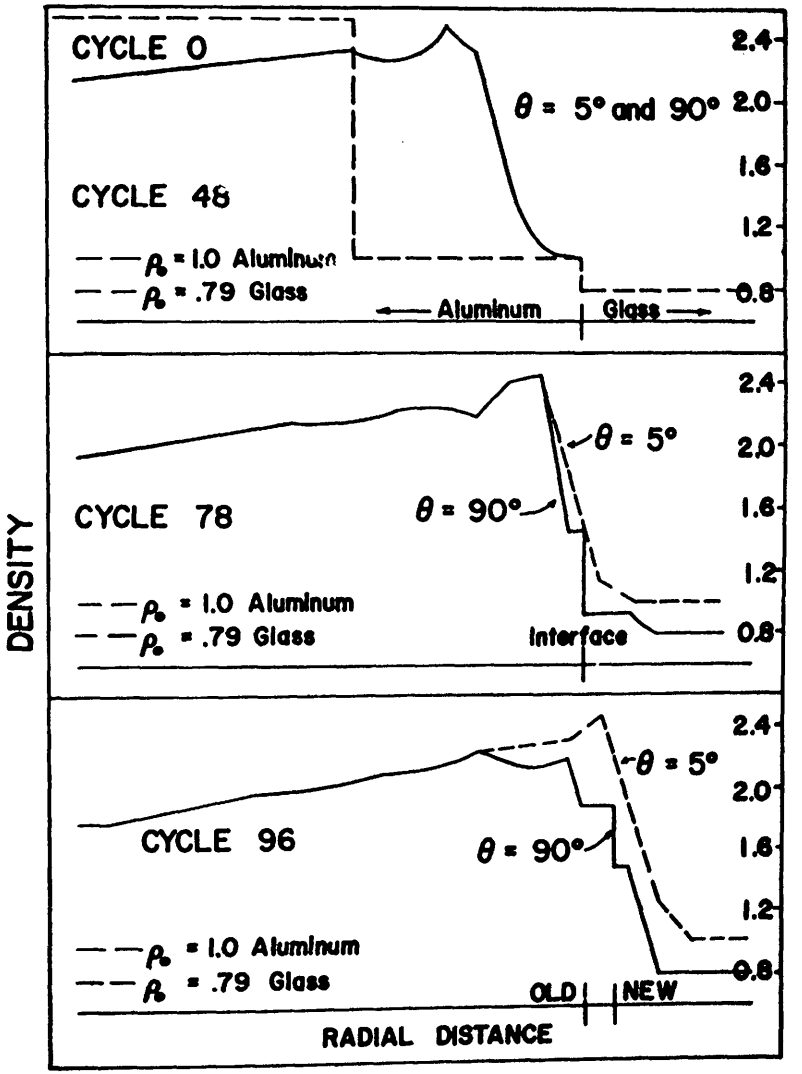

Fig. 8. Propagation of Density Front.

LITERATURE CITED

Beard, D. 1961 (Jan.). Solid interplanetary matter. Sandia Corporation, SCR-252.

Bethe, H. A. 1942. The theory of shock waves for an arbitrary equation of state. OSRD No. 545 (Division B of National Defense Research Committee).

Bjork, R. L. 1958. Effects of a meteoroid impact on steel and aluminum in space. Engineering Division, Rand Corporation, P-1662.

Collins, R. D., Jr. and W. Kinard. 1960 (May). NASA TN D-230.

Grüneisen, E. 1926. Zustand der Festen Körpers, in "Handbuch der Physik", vol. 10, Julius Springer, Berlin, p. 1-52 (Translation by S. Reiss, NASA republication RE 2-18-59w, Feb., 1959).

Landshoff, R. 1955 (Jan.). A numerical method for treating fluid flow in the presence of shocks. Los Alamos Scientific Laboratory, LA-1930.

Longley, H. J. 1959 (Apr.). Methods of differencing in Eulerian hydrodynamics. Los Alamos Scientific Laboratory, LAMS-2379.

Summers, J. L. 1959 (Oct.). NASA TN D-94.

Todd, F. C., H. R. Lake and B. A. Sodek, Jr. 1960 (Dec.). Progress report No. 1, contract NASr-7, Oklahoma State University Research Foundation.

Todd, F. C., Shi-yu Wu, H. R. Lake and B. A. Sodek, Jr. 1961 (Mar.). Progress report no. 2, Contract NASr-7, Oklahoma State University Research Foundation.

von Neumann, J., and R. D. Richtmyer. 1950. A method for the numerical calculations of hydrodynamical shocks. J. Appl. Phys. 21: 232-237.

Wackerle, J. 1962. Shock wave compression of quartz. J. Appl. Phys. 33: 922-37.

Walsh, J. M., N. H. Rice and R. G. McQueen. 1958. Compression of solids by strong shock waves. Solid State Physics, Advances in Research and Applications, 6: 1-63, Academic Press, New York, N.Y.